

# Varying the forcing scale in low Prandtl number dynamos

A. Brandenburg<sup>1,2,3,4\*</sup>, N. E. L. Haugen<sup>5,6</sup>, Xiang-Yu Li<sup>1,2,7</sup> and K. Subramanian<sup>8</sup>

<sup>1</sup>Laboratory for Atmospheric and Space Physics, University of Colorado, Boulder, CO 80303, USA

<sup>2</sup>Nordita, KTH Royal Institute of Technology and Stockholm University, 10691 Stockholm, Sweden

<sup>3</sup>JILA and Department of Astrophysical and Planetary Sciences, University of Colorado, Boulder, CO 80303, USA

<sup>4</sup>Department of Astronomy, Stockholm University, SE-10691 Stockholm, Sweden

<sup>5</sup>SINTEF Energy Research, 7465 Trondheim, Norway

<sup>6</sup>Department of Energy and Process Engineering, NTNU, 7491 Trondheim, Norway

<sup>7</sup>Department of Meteorology and Bolin Centre for Climate Research, Stockholm University, Stockholm, Sweden

<sup>8</sup>Inter University Centre for Astronomy and Astrophysics, Post Bag 4, Pune University Campus, Ganeshkhind, Pune 411 007, India

17 January 2022, Revision: 1.87

## ABSTRACT

Small-scale dynamos are expected to operate in all astrophysical fluids that are turbulent and electrically conducting, for example the interstellar medium, stellar interiors, and accretion disks, where they may also be affected by or competing with large-scale dynamos. However, the possibility of small-scale dynamos being excited at small and intermediate ratios of viscosity to magnetic diffusivity (the magnetic Prandtl number) has been debated, and the possibility of them depending on the large-scale forcing wavenumber has been raised. Here we show, using four values of the forcing wavenumber, that the small-scale dynamo does not depend on the scale-separation between the size of the simulation domain and the integral scale of the turbulence, i.e., the forcing scale. Moreover, the spectral bottleneck in turbulence, which has been implied as being responsible for raising the excitation conditions of small-scale dynamos, is found to be invariant under changing the forcing wavenumber. However, when forcing at the lowest few wavenumbers, the effective forcing wavenumber that enters in the definition of the magnetic Reynolds number is found to be about twice the minimum wavenumber of the domain. Our work is relevant to future studies of small-scale dynamos, of which several applications are being discussed.

**Key words:** dynamo — MHD – magnetic fields — turbulence — Sun:dynamo

## 1 INTRODUCTION

Magnetic fields are ubiquitous in astrophysics. In fact, most of the gas in the universe is ionized and therefore electrically conducting. This allows part of the kinetic energy of the gas to be converted into magnetic energy through the dynamo instability. This is when the induction equation, which is linear in the magnetic field  $\mathbf{B}$ , has exponentially growing solutions, starting from just a weak seed magnetic field. A linear evolution equation can also be formulated for the two-point correlation function,  $\langle B_i(\mathbf{x})B_j(\mathbf{x} + \mathbf{r}) \rangle$ , where angle brackets denote averaging, for example over volume,  $\mathbf{x}$  is the position vector, and  $\mathbf{r}$  the separation between the two points. Depending on the statistics of the velocity field and the electric conductivity, this equation may have exponentially growing solutions. In that case, we talk about a small-scale dynamo instability, where  $\langle \mathbf{B}^2 \rangle$  grows exponen-

tially, in contrast to a large-scale dynamo instability where  $\langle \mathbf{B} \rangle$  itself grows exponentially.

The first rigorous derivation of exponentially growing solutions for  $\langle \mathbf{B}^2 \rangle$  in statistically mirror-symmetric homogeneous turbulence goes back to the early work of Kazantsev (1968), but it was not until direct numerical simulations since Meneguzzi et al. (1981) started seeing small-scale dynamo action on the computer that this work became more widely known. Subsequent work, notably by Kulsrud & Anderson (1992), Subramanian (1999), and Boldyrev et al. (2005), have significantly contributed to our understanding of small-scale dynamos and their interaction with large-scale ones; see the review by Brandenburg et al. (2012). In particular, the presence of flows which allow for a large-scale dynamo may also ease the excitation of the small-scale dynamo. This, however, always requires some departure from the most generic form of turbulence, which is isotropic, homogeneous, and statistically mirror-symmetric. Thus, a small-scale dynamo is a generic feature of any tur-

\* E-mail: brandenb@nordita.org

bulence in electrically conducting gases or fluids, because it is able to produce dynamically important magnetic energy densities comparable to the kinetic energy density. This is when the velocity begins to depend on  $\mathbf{B}$  and the induction equation is no longer linear in  $\mathbf{B}$ , leading to dynamo saturation. Such a state can be regarded as a generalization of standard Kolmogorov turbulence to an ionized gas or fluid that is electrically conducting and therefore subject to the small-scale dynamo instability. However, how generic this generalization of standard Kolmogorov turbulence really is depends on how generic is this dynamo instability.

Already over 20 years ago, analytic work showed that the dynamo threshold of the small-scale (also known as fluctuation dynamo; see Schekochihin et al. 2007; Eyink 2010; Bhat & Subramanian 2013) increases with decreasing magnetic Prandtl number (Rogachevskii & Kleeorin 1997), i.e., the ratio  $\text{Pr}_M = \nu/\eta$  of fluid viscosity  $\nu$  to magnetic diffusivity  $\eta$ . In the interstellar medium, where the density is very low, we have  $\text{Pr}_M \gg 1$ , but in stars, and even in their outer layers, we have  $\text{Pr}_M \ll 1$ . The increase of the dynamo threshold with decreasing  $\text{Pr}_M < 1$  was then confirmed numerically by Schekochihin et al. (2004, 2005) and Haugen et al. (2004). By solving the Kazantsev (1968) equation, Schober et al. (2012) confirmed the increased critical value of  $\text{Re}_M$  both for Kolmogorov and Burgers turbulence. From a technical point of view, the problem is doubly difficult. On the one hand, as we decrease  $\text{Pr}_M$ , even when keeping the magnetic Reynolds number and therefore  $\eta$  unchanged, we already need more numerical resolution because  $\nu$  decreases and therefore the fluid Reynolds number increases. On the other hand, if the dynamo threshold is increasing, one must increase the magnetic Reynolds number for the dynamo to remain supercritical, demanding even higher fluid Reynolds numbers and therefore even higher numerical resolution.

The increase of the dynamo threshold was interpreted as being a consequence of the scale where the magnetic spectrum peaks during the kinematic stage, moving away from the viscous subrange into the inertial range of the turbulence where the velocity field becomes rougher (Boldyrev & Cattaneo 2004). Here, rougher means that velocity differences  $v_l$  between two points separated by  $l$ , scale as  $v_l \propto l^\alpha$  with  $\alpha < 1$ . However, we have known for some time that, just before exiting the inertial range, the kinetic energy spectrum becomes even shallower. This is generally known as the spectral bottleneck effect (She & Jackson 1993). It is theoretically explained as a consequence of a reduced efficiency of triad interactions with modes in the viscous subrange (Falkovich 1994). This has consequences for the dynamo threshold. It makes the velocity even rougher than for Kolmogorov turbulence (which has  $\alpha = 1/3$ ) near the bottleneck region of the spectrum. Subsequent work of Iskakov et al. (2007) showed that this particular problem of the small-scale dynamo suffering from the spectral bottleneck can be overcome by decreasing the magnetic Prandtl number even further. The most difficult case is  $\text{Pr}_M \approx 0.1$ , where the excitation conditions were so high that nobody was able to confirm that the small-scale dynamo could be excited. Iskakov et al. (2007) found supercritical solutions near  $\text{Pr}_M \approx 0.1$  when using hyperviscosity in their simulations, which does however affect the strength of the spectral bottleneck, as will be discussed in a moment. Even the re-

cent convection simulations of Käpylä et al. (2018) at a resolution of  $1024^3$  meshpoints found only decaying magnetic fields at  $\text{Pr}_M = 0.1$ .

In the meantime, two further developments have occurred. On the one hand, in the nonlinear regime the case  $\text{Pr}_M = 0.1$  turned out to be not so difficult as in the kinematic dynamo regime and sustained dynamo action has been found. This could be explained by the spectral bottleneck being suppressed by a dynamically important magnetic field; see Fig. 2 of Brandenburg (2011) for  $\text{Pr}_M = 0.05$  and  $0.02$ . For  $\text{Pr}_M = 1$ , on the other hand, the bottleneck is not yet strongly suppressed; see Fig. 2 of Haugen & Brandenburg (2006). On the other hand, even in the kinematic (linear) problem, Subramanian & Brandenburg (2014, hereafter SB14) found small-scale dynamo action at  $\text{Pr}_M = 0.1$  in their simulations where turbulence was being forced at a wavenumber of about four, instead of one to two, which had been used in all the small-scale dynamo studies until then. This raised the new possibility that maybe the spectral bottleneck itself could be an artifact of having forced the turbulence at or near the scale of the domain. Clarifying this question is the main goal of the present paper.

An artificially enhanced bottleneck effect has been seen in simulations that use hyperviscosity instead of the regular diffusion operator proportional to  $\nabla^2$ . Biskamp & Müller (2000) found that this artificially produced bottleneck effect could also modify the entire inertial range, but this was not confirmed in subsequent simulations (Haugen & Brandenburg 2006). Furthermore, Donzis & Sreenivasan (2010) have presented evidence that the bottleneck becomes less strong at higher Reynolds numbers. It is therefore perhaps fair to say that the physical reality of the bottleneck effect is not universally accepted, because it is not easily seen in high Reynolds number wind tunnel turbulence and in atmospheric turbulence (Tsuji 2004). This is because in wind tunnel turbulence, one only measures a one-dimensional spectrum. For pure power laws, one- and three-dimensional power spectra are identical, but this is not the case near the breakpoint of the dissipative subrange, where the  $k^{-5/3}$  power law changes sharply into an exponential fall-off. This causes the bottleneck effect to be greatly diminished in a one-dimensional projection (Dobler et al. 2003). Thus, we argue that the bottleneck effect is physically real for the Reynolds numbers under consideration, but that it is less strong than what is caused by hyperviscosity and it is usually barely noticeable in one-dimensional measurements. Furthermore, even though Donzis & Sreenivasan (2010) find the bottleneck becoming weaker at larger Reynolds number, this happens slowly and even for a Reynolds number of 1000 based on the Taylor microscale, the bottleneck is still rather prominent.

The astrophysical significance of the spectral bottleneck effect lies in the effect it might potentially have on the numerical study of small-scale dynamos, at small and moderate  $\text{Pr}_M < 1$ . Since these are dynamos that operate on the resistive length scale, they depend on the small-scale properties of the flow. Although these scales are in reality very small, this is usually not the case in most of the numerical simulations that much of our intuition has to rely upon; see Cattaneo (1999) and Thaler & Spruit (2015) for a discussion of small-scale dynamos operating near the solar surface.

Specifically, in this paper, we want to address the possibility that the kinematic small-scale turbulent dynamo at low magnetic Prandtl number might depend on the forcing scale. We consider Run g01 of SB14 which had  $\text{Pr}_M = 0.1$  and a magnetic Reynolds number of 200, so the fluid Reynolds number was 2000. They used  $512^3$  meshpoints, so our first question is whether this resolution was adequate. We begin by rerunning their case at a higher resolution of  $1152^3$  meshpoints. We then consider smaller values of the forcing wavenumber, keeping however the values of  $\nu$  and  $\eta$  unchanged.

## 2 THE MODEL

Similar to SB14, we consider dynamo action in a cubic domain of size  $L_1^3$ , driven by turbulence forced at normalized wavenumbers  $k_f/k_1$  ranging from 1.5 to 4, where  $k_1 = 2\pi/L_1$  is the smallest wavenumber in the domain. However, unlike SB14, we consider only nonhelical forcing, so no large-scale dynamo of  $\alpha^2$  type is possible (Moffatt 1978). We are only interested in the early exponential growth or decay phase and therefore omit the Lorentz force in the momentum equation. We consider an isothermal compressible gas and thus solve the following hydromagnetic evolution equations for the magnetic vector potential  $\mathbf{A}$ , the velocity  $\mathbf{u}$ , and the density  $\rho$ ,

$$\frac{\partial}{\partial t} \mathbf{A} = \mathbf{u} \times \mathbf{B} - \eta \mu_0 \mathbf{J}, \quad (1)$$

$$\frac{D}{Dt} \mathbf{u} = -c_s^2 \nabla \ln \rho + \mathbf{f} + \rho^{-1} \nabla \cdot 2\nu \rho \mathbf{S}, \quad (2)$$

$$\frac{D}{Dt} \ln \rho = -\nabla \cdot \mathbf{u}, \quad (3)$$

where  $\mathbf{B} = \nabla \times \mathbf{A}$  is the magnetic field,  $\mathbf{J} = \nabla \times \mathbf{B}/\mu_0$  is the current density,  $\mu_0$  is the vacuum permeability,  $c_s = \text{const}$  is the isothermal sound speed,  $D/Dt = \partial/\partial t + \mathbf{u} \cdot \nabla$  is the advective time derivative,  $\mathbf{S}$  is the traceless rate-of-strain tensor with components  $S_{ij} = \frac{1}{2}(u_{i,j} + u_{j,i}) - \frac{1}{3}\delta_{ij} \nabla \cdot \mathbf{u}$ , and commas denote partial derivatives. Energy supply is provided by the forcing function  $\mathbf{f} = \mathbf{f}(\mathbf{x}, t)$ , which is random in time and defined as

$$\mathbf{f}(\mathbf{x}, t) = \text{Re}\{N \mathbf{f}_{\mathbf{k}(t)} \exp[i\mathbf{k}(t) \cdot \mathbf{x} + i\phi(t)]\}, \quad (4)$$

where  $\mathbf{x}$  is the position vector. The wavevector  $\mathbf{k}(t)$  and the random phase  $-\pi < \phi(t) \leq \pi$  change at every time step, so  $\mathbf{f}(\mathbf{x}, t)$  is  $\delta$ -correlated in time. Therefore, the normalization factor  $N$  has to be proportional to  $\delta t^{-1/2}$ , where  $\delta t$  is the length of the time step. On dimensional grounds it is chosen to be  $N = f_0 c_s (|\mathbf{k}| c_s / \delta t)^{1/2}$ , where  $f_0$  is a nondimensional forcing amplitude. We choose  $f_0 = 0.02$ , which, for our range of Reynolds numbers, results in a maximum Mach number of about 0.5 and an rms velocity of about 0.13, which is almost the same for all the runs. At each timestep we select randomly one of many possible wavevectors in a certain range around a given forcing wavenumber with average value  $k_f$ .

Our model is governed by several nondimensional parameters. In addition to the scale separation ratio  $k_f/k_1$ , introduced above, there are the magnetic Reynolds and Prandtl numbers

$$\text{Re}_M = u_{\text{rms}}/\eta k_f, \quad \text{Pr}_M = \nu/\eta. \quad (5)$$

**Table 1.** Parameters of Runs A–D2 at  $1152^3$  meshpoints and comparison with Run g01 of SB14 and D3 at  $512^3$  meshpoints. Here,  $k_f = k_f/k_1$ ,  $\tilde{\epsilon}_{-4}^K = \epsilon_K/(10^{-4} c_s^3 k_1)$ ,  $\tilde{u}_{\text{rms}} = u_{\text{rms}}/c_s$ ,  $\tilde{\lambda}_{-3} = \lambda/(10^{-3} c_s k_1)$ , and  $\tilde{k}_\nu = k_\nu/k_1$ .

Run	$\tilde{k}_f$	$\tilde{\epsilon}_{-4}^K$	$\tilde{u}_{\text{rms}}$	$\text{Re}_M$	$\tilde{\lambda}_{-3}$	$\tilde{k}_\nu$	$a_K$	$a_\eta$
g01	4.06	3.38	0.127	196	2.9	—	—	—
A	4.06	3.39	0.128	197	2.5	536	1.00	1.05
B	3.13	2.85	0.129	258	3.1	514	1.00	1.02
C	2.23	1.91	0.128	359	4.6	465	0.95	1.03
D	1.54	1.46	0.132	536	4.2	435	0.95	1.00
D2	1.54	1.39	0.126	178	−1.9	194	—	—
D3	1.54	1.33	0.131	284	1.9	265	—	—

These two numbers also define the fluid Reynolds number,  $\text{Re} = u_{\text{rms}}/\nu k_f = \text{Re}_M/\text{Pr}_M$ . The maximum values that can be attained are limited by the numerical resolution and become more restrictive at larger scale separation. The calculations have been performed using the PENCIL CODE<sup>1</sup> at a resolution of  $1152^3$  mesh points, except for Run D3 where  $512^3$  mesh points were used.

## 3 SIMULATIONS

In the following we present runs for  $\text{Pr}_M = 0.1$  with different forcing wavenumbers  $k_f$ , where  $k_f/k_1$  ranges from 4.06 (the value used in SB14) down to 1.54 (the averaged value for all the 20 wavevectors with lengths between 1 and  $\sqrt{3}$ ; see Table 1.) We determine the growth rate  $\lambda$  by plotting the logarithm of the root-mean-square magnetic field,  $\ln B_{\text{rms}}$ , versus time in sound travel times,  $t c_s k_1$ . The instantaneous growth rate is  $\lambda(t) = d \ln B_{\text{rms}}/dt$ . To have values of the logarithm close to zero, we normalize by an arbitrarily chosen reference value,  $B_{\text{ref}}$ . Statistical errors have been determined as the largest departure of any one third of that part of time series where the data is deemed to be in a steady state.

It turns out that for  $k_f/k_1 = 4.06$ , the growth rate is within 3% the same as that found by SB14; compare the red line in Fig. 1 with the orange line for Run g01. This is small enough so that we can conclude that their resolution was adequate. Nevertheless, we keep this higher resolution for the following study.

We then proceed to lower values of  $k_f$ . We expected that at some value the dynamo would cease to be excited. However, it turned out that, some time after restarting from an earlier run with larger  $k_f$ , a clear exponential growth commenced where the growth rate was even larger than before; see again Fig. 1. Note, however, that it always takes some hundred sound travel times to establish exponential small-scale dynamo growth. This time corresponds to 7–8 turnover times when based on the values of  $u_{\text{rms}}$  and  $k_f = 1.54 k_1$  for Run D, and about 30 turnover times when  $k_f \approx 4$  for Run A.

Of course, given that  $\eta$  was unchanged for Runs A–D, and  $k_f$  and  $u_{\text{rms}}$  enter in the definition of  $\text{Re}_M$ , the values of  $\text{Re}_M$  increase; see Table 1. Thus, since Run D now turns out to be clearly supercritical, we can conclude that the

<sup>1</sup> <https://github.com/pencil-code>

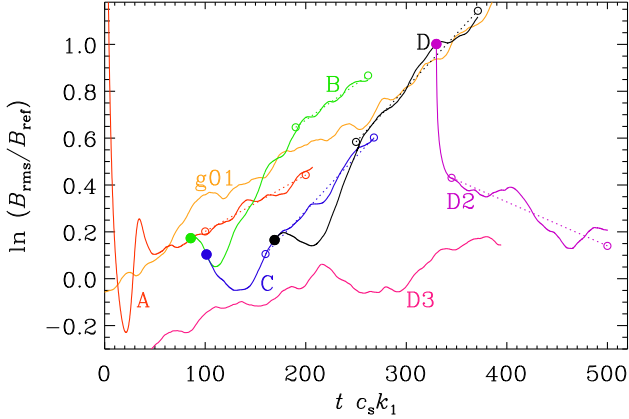


**Figure 1.** Time series of  $B_{\text{rms}}$  (normalized by an arbitrarily chosen  $B_{\text{ref}}$ ) for Runs A–D and comparison with Run g01 of SB14 (orange). Except for Run A, which was started from scratch, Runs B–D have been restarted at the times indicated by a filled circle. Run D2 (pink) has been restarted with a smaller value of  $\text{Re}_M$  close to that of Run A. The dotted lines with open circles on their end points indicate the least-square fit to the last part of the curves indicated. Run D3 has been restarted from Run f01 of SB14 and averaging has been performed over 800 sound travel times (not indicated).

critical value of  $\text{Re}_M$  for the small-scale dynamo at small  $k_f$  is clearly below 500. This is compatible with the simulations of Iskakov et al. (2007), whose largest value of  $\text{Re}_M$  was 450 based on the wavenumber  $k_1$  of the domain, and therefore around 300 when based on  $k_f$  (with  $k_f = \sqrt{2} k_1$  in their case), which is the normalization used in the present paper.

Runs A and D2 have nearly the same  $\text{Re}_M$ , but their growth rates are not the same. These two runs do have different values of  $k_f/k_1$ , so there could be an additional dependence on the scale separation ratio. On the other hand, these two data points still fit reasonably well onto a linear dependence of  $\lambda/u_{\text{rms}} k_f$  versus  $\text{Re}_M$ ; see the top panel of Fig. 2. This suggests that the possibility of an additional  $k_f$  dependence is probably not real. Specifically, we find

$$\lambda/u_{\text{rms}} k_f \approx (\text{Re}_M - \text{Re}_M^{\text{crit}})/13,000 \quad (6)$$

with  $\text{Re}_M^{\text{crit}} \approx 200$ . Furthermore, the largest two data points would be compatible with the theoretically expected square root dependence,

$$\lambda/u_{\text{rms}} k_f \approx 10^{-3} \text{Re}_M^{1/2} \quad (\text{for large } \text{Re}_M). \quad (7)$$

We also point out that for all these runs, the value of the dissipation rate,  $\epsilon_K = \langle 2\nu \rho \mathbf{S}^2 \rangle$ , scales well with the theoretical dependence proportional to  $u_{\text{rms}}^3 k_f$  ( $\epsilon_K \approx 0.04 u_{\text{rms}}^3 k_f$ ). Alternatively, for low  $\text{Pr}_M$  dynamos, Kleorin & Rogachevskii (2012) proposed a logarithmic dependence  $\propto \ln(\text{Re}_M/\text{Re}_M^{\text{crit}})$ . Specifically, we find

$$\lambda/u_{\text{rms}} k_f \approx 0.023 \ln(\text{Re}_M/\text{Re}_M^{\text{crit}}) \quad (8)$$

as a reasonable fit.

Let us now discuss the question how to resolve the apparent conflict between our value of  $\text{Re}_M^{\text{crit}} \approx 200$  and that of around 300 obtained by Iskakov et al. (2007) for a supercritical  $\text{Pr}_M = 0.1$  dynamo. First, they only quote growth for  $\text{Re}_M = 450/\sqrt{2} \approx 320$  and decay for  $\text{Re}_M = 230/\sqrt{2} \approx 160$ .

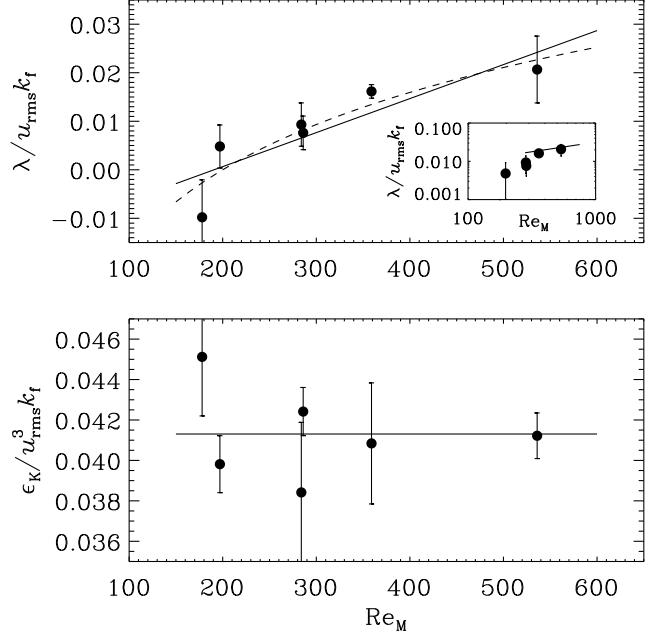


**Figure 2.** Growth rate (top) and energy dissipation rate (bottom) versus magnetic Reynolds number. In the top panel, the solid and dashed lines refer to Equations (6) and (8), respectively. The inset shows a comparison with the theoretically expected  $\text{Re}_M^{1/2}$  (straight line) scaling in a double-logarithmic representation. In the lower panel, the horizontal line gives the average value of 0.040.

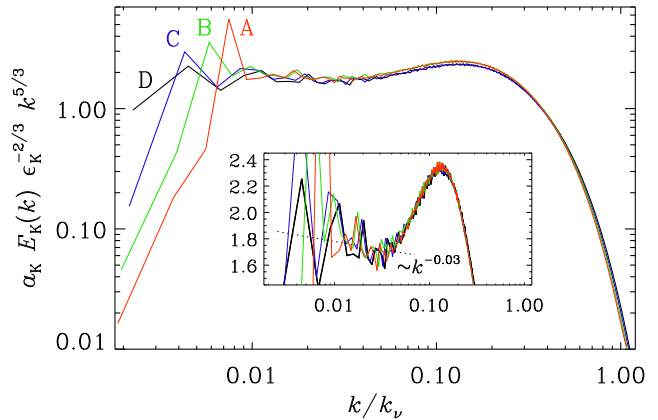


**Figure 3.** Compensated kinetic energy spectra for all four runs. The inset shows the compensated spectra on a linear scale. The dotted line shows the theoretically expected inertial range correction proportional to  $k^{-0.03}$ .

Second, interpolating between Runs D and D2 would yield  $\text{Re}_M^{\text{crit}} \approx 290$ , which is close to the value of Iskakov et al. (2007). Interpolating between Runs D2 and D3 would yield  $\text{Re}_M^{\text{crit}} \approx 230$ , but Run D3 has lower resolution and may be unreliable. Furthermore, looking again at Fig. 1, it is clear that there can sometimes be extended intervals during which the instantaneous growth rate can be significantly different. It may however be noted that for  $\text{Pr}_M = 1$ , the discrepancy is smaller in that Iskakov et al. (2007) found  $\text{Re}_M^{\text{crit}} \approx 60/\sqrt{2} = 42$  while Haugen et al. (2004) found  $\approx 35$ .



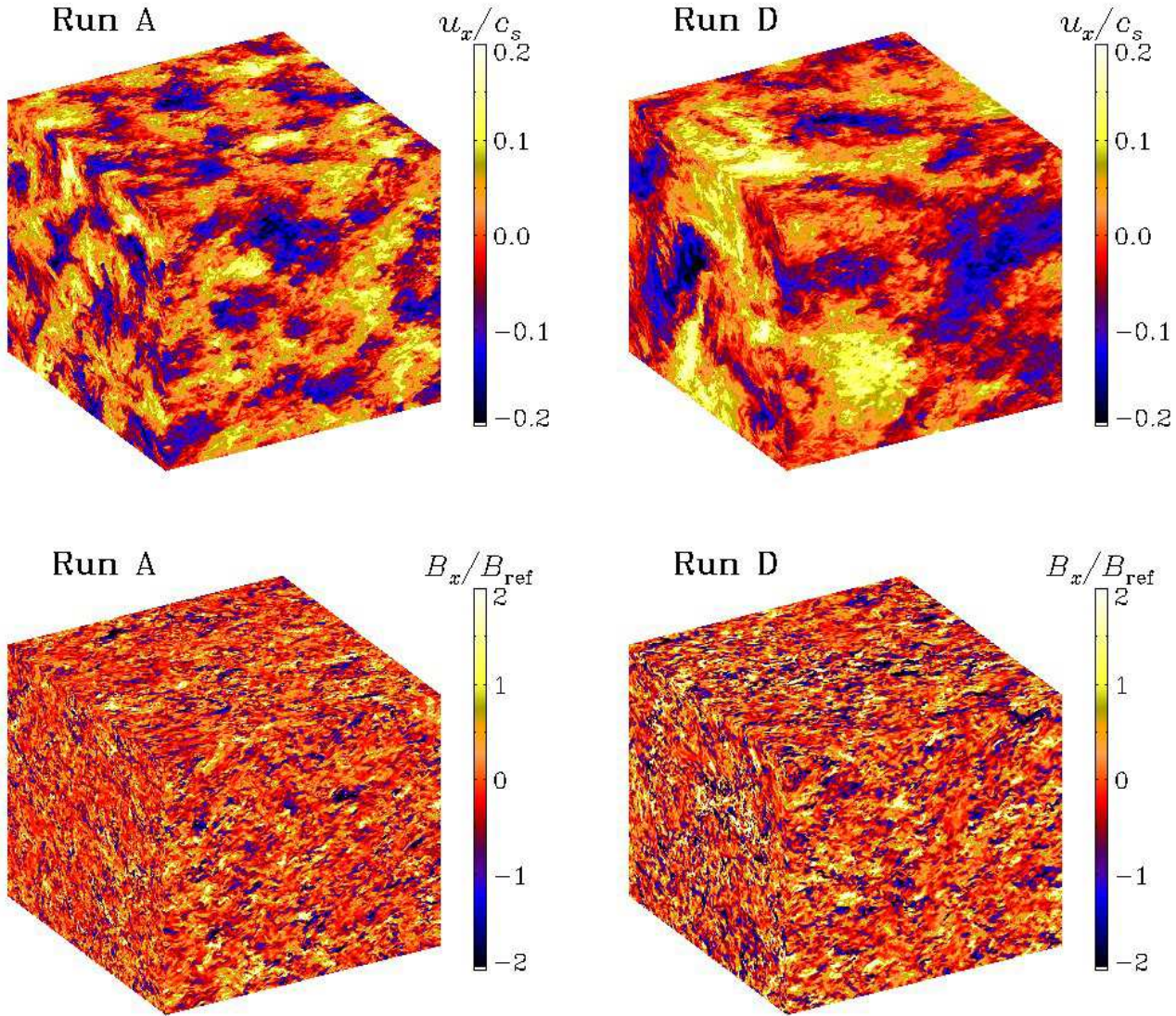


**Figure 4.** Visualizations of  $u_x$  (top) and  $B_x$  (bottom) for Runs A (left) and D (right) on the periphery of the domain at the last time of each run.

Third, and this is perhaps the simplest explanation, the effective value of  $k_f$  may not be equal to the nominal average given by  $k_f = 1.54 k_1$ , but it may be by up to 300/200 times larger. Indeed, if we were to declare that  $k_f \rightarrow k_f^{\text{eff}} \approx 2 k_1$  for Run D2, it would also resolve the otherwise increasing discrepancy between Runs A and D2, which have similar nominal  $\text{Re}_M$ , but different growth rates. We therefore propose  $\text{Re}_M^{\text{crit}} \approx 200$  as the currently best value for the small-scale dynamo at  $\text{Pr}_M = 0.1$ .

Next, we study whether the height of the bottleneck was affected as we changed  $k_f$  from 4.06 to 1.54. The results for the kinetic energy spectra, time-averaged over the statistically steady state, are shown in Fig. 3. These spectra have been compensated by  $\epsilon_K^{-2/3} k^{5/3}$ . There we see a short plateau corresponding to the inertial range with a value (known as the Kolmogorov constant) of around 1.7, close to that found by Donzis & Sreenivasan (2010). The

wavenumber on the abscissa has been scaled by the dissipative Kolmogorov cutoff wavenumber,  $k_\nu = (\epsilon_K/\nu^3)^{1/4}$ . However, in order to achieve ever better overlap between the different spectra, we have applied an additional scaling factor  $a_K$  close to unity, whose values are listed in Table 1 for each of the four runs.

All four curves are seen to collapse perfectly on top of each other at high wavenumbers. We can thus conclude that the spectral bottleneck is insensitive to the details of the large-scale forcing. This appears plausible, but it was never demonstrated and SB14 were clearly concerned about this aspect, which is why they considered, for safety reasons, the value  $k_f/k_1 \approx 4$  instead of just 1.54. But now we know that this would not have been necessary and that they could have reached even larger values of  $\text{Re}_M$  by lowering  $k_f$ . However, their findings concerning the small-scale dynamo emerged as a by-product while studying the kinematic  $\alpha^2$  large-scale

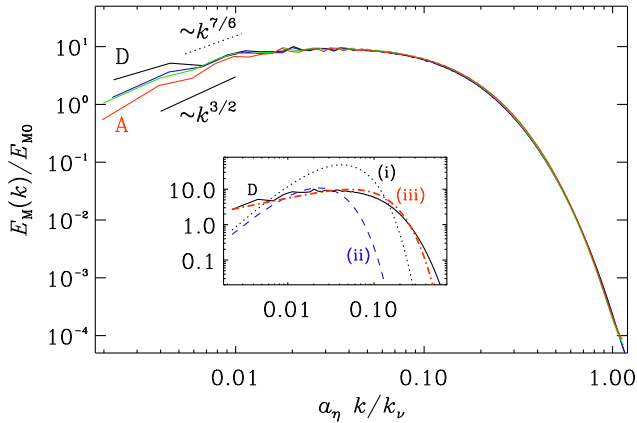


**Figure 5.** Magnetic energy spectra for all four runs, time-averaged after compensating against the exponential growth, as explained in the text. The coloring of the lines is the same as in Figs. 1 and 3. The inset shows a comparison between the magnetic spectrum for Run D and the Macdonald function with different arguments explained in the text.

dynamo in the presence of helicity. The fastest growing mode of this dynamo occurs at  $k < k_f/2$ , which justified their choice of  $k_f/k_1 \approx 4$  in those cases.

The inset of Fig. 3 shows more clearly the relevant part of the inertial range and the bottleneck. The height of the bottleneck is roughly compatible with what was found by Kaneda et al. (2003) using incompressible hydrodynamic turbulence simulations at a resolution of  $4096^3$  meshpoints. We also see that an inertial range correction of about  $k^{-0.03}$ , as expected from the intermittency model of She & Leveque (1994), is compatible with the data. This is indicated in the inset of Fig. 3 by the dotted line. Note, however, that the simulations of Kaneda et al. (2003) and also those of Haugen & Brandenburg (2006) showed a steeper inertial range correction of about  $k^{-0.1}$ , which is not theoretically expected.

In Fig. 4 we compare visualizations of velocity and magnetic field for Runs A and D. For both fields, we show the  $x$ -component on the periphery of the domain. For both fields, the visual impression is dominated by the largest structures, especially for the velocity field. One sees that the smallest structures of the magnetic field tend to cluster in particular regions in space, especially for Run D. Nevertheless, the scale of the magnetic structures seems the same in both cases.

To verify the visual impression regarding the similarity in scales, we show in Fig. 5 magnetic power spectra,  $E_M(k)$ , which have been averaged after compensating against the exponential growth with a factor of  $\exp(-\lambda t)$ , where the values of  $\lambda$  are listed in Table 1. The total magnetic energy,  $E_{M0} = \int E_M(k) dk$  is used for normalization. The results shown in Fig. 5 demonstrate again perfect agreement between all the spectra at sufficiently large values of  $k$ . Again, to achieve better overlap between the different spectra, we have applied an additional scaling factor  $a_\eta$  on the abscissa. Their values are listed in Table 1. Note, however, that the theoretically expected  $k^{3/2}$  scaling seen in simulations with larger values of  $\text{Pr}_M$  (Haugen et al. 2004) applies at best only to Run A, and this only over a rather short range. A

shallower  $k^{7/6}$  scaling was proposed by SB14 and Bhat et al. (2016), but even that appears still too steep for Run D; see Fig. 5.

For  $\text{Pr}_M \gg 1$ , the theoretically expected eigenfunction is proportional to  $k^{3/2} K_\nu(k/k_\eta)$  with index  $\nu = 0$  and  $k_\eta/k_1 = (R_m/6)^{1/2} \approx 9$  (Kulsrud & Anderson 1992; Schekochihin et al. 2002). This was found to provide a good fit to the numerical simulation of Brandenburg and Subramanian (2005). For low  $\text{Pr}_M$ , the functional form yields a much more extended  $k^{3/2}$  range than what is seen in the present simulation; see (i) in the inset of Fig. 5. Lowering it to  $k_\eta/k_1 = 5$  fits the low  $k$  range better, but provides a poor description for large  $k$  (ii). A better overall description is given by  $\nu = 2$  and  $k_\eta/k_1 = (R_m/1.4)^{1/2} \approx 20$ ; see (iii) in the inset of Fig. 5.

Finally, let us ask if the above results on the low  $\text{Pr}_M$  dynamo can be understood based on general arguments? We recall that in the bottleneck region, the spectrum becomes shallower and the velocity becomes even more rough than for a pure Kolmogorov spectrum. Suppose this occurs at a wavenumber around  $k_B = f k_\nu$ . At low  $\text{Pr}_M$ , the turbulent flow with the resistive scale  $k_\eta$  around  $k_B$ , will be expected to fail to be a dynamo. In fact, from the Kazantsev (1968) analysis one knows that a rough velocity with turbulent diffusion  $v_l l \propto l^{1+\alpha}$  and  $\alpha < 0$ , fails to be a dynamo (Boldyrev & Cattaneo 2004). This would happen if the resistive scale falls in the bottleneck region. For a Kolmogorov spectrum, we have  $k_\eta \sim k_f \text{Re}_M^{3/4}$ , while  $k_\nu \sim k_f \text{Re}^{3/4}$ , and thus we expect the low  $\text{Pr}_M$  dynamo to be difficult to excite when  $k_\eta = k_f \text{Re}_M^{3/4} = k_B = f k_\nu = f k_f \text{Re}^{3/4}$ , or when  $\text{Pr}_M = \text{Re}_M/\text{Re} \sim f^{4/3}$ , independent of  $k_f$ . From Fig. 3 we see that the rising part of the bottleneck region, where one expects  $\alpha \sim 0$ , occurs at a wavenumber  $\sim 0.1 k_\nu$ , which gives  $f \sim 0.1$ , implying for the critical  $\text{Pr}_M \sim 0.05$ . This is indeed roughly the value of  $\text{Pr}_M$  where it has been difficult to excite a small-scale dynamo. The above argument also shows that such a difficulty should not arise for either a much smaller or larger  $\text{Pr}_M$ .

## 4 CONCLUSIONS

Our work has conclusively demonstrated that the inertial range and the spectral bottleneck of turbulence are not affected by the details of the forcing at large length scales, specifically the value of  $k_f$ . We have also shown that the value of  $k_f$  affects neither the excitation condition of the small  $\text{Pr}_M$  dynamo nor the shape of the exponentially growing magnetic energy spectrum at moderate to large values of the wavenumber. This is significant for future studies of small-scale dynamos in that it can now be regarded as safe to use the smallest possible forcing wavenumber in order to maximize the extent of the inertial range. Clearly, this conclusion does not carry over to other types of dynamos, notably the large-scale dynamos, where a minimal forcing wavenumber of about three was found to be just acceptable (Brandenburg et al. 2008).

We have changed  $k_f$  only by a factor of less than three, so we cannot make any claims about larger ranges. However, when changing  $k_f$  from  $4.06 k_1$  (where 210 different  $\mathbf{k}$  vectors contribute in the range  $3.5 < |\mathbf{k}|/k_1 < 4.5$ ) to the smallest possible value of  $1.54 k_1$  (where only 20 vectors contribute

in  $1.4 < |\mathbf{k}|/k_1 < 1.8$ ), we have not seen any systematic changes in the velocity spectrum. The changes in the growth rate appear to be well explained by the expected variation of  $\text{Re}_M$ . For  $k_f = 1.54 k_1$ , however, we have argued that the effective forcing wavenumber is  $k_f^{\text{eff}} \approx 2 k_1$ . It would be of interest to extend our work to values of  $\text{Pr}_M$  well below 0.1, to see whether one can find an asymptotic regime where  $\text{Re}_M^{\text{crit}}$  becomes independent of  $\text{Pr}_M$ . At the present time, this would be an expensive task, but the day will come when this can easily be done.

We have seen that for  $\text{Pr}_M = 0.1$ , the shape of the magnetic energy spectrum is clearly different from that at large  $\text{Pr}_M$ . It is shallower at large wavenumbers and not proportional to  $k^{3/2}$ , as already noted earlier (Bhat et al. 2016). Although Kleorin & Rogachevskii (2012) have obtained the real space eigenfunction in various asymptotic domains for this case in analytic form, it still remains to be shown how the spectrum actually looks like.

Further work on small-scale dynamos remains manifold. For example, compressibility effects in general and the Mach number dependence are important (Haugen et al. 2004; Federrath et al. 2011, 2014; Sur et al. 2018) and would be interesting to reconsider at high resolution using direct numerical simulations. There are also questions regarding the importance of small-scale dynamo-generated magnetic fields in enhancing the effective turbulent viscosity, for example in the Sun's convection zone. Small-scale dynamo-produced magnetic fields may also modify the values of turbulent transport coefficients, such as turbulent diffusivity and the  $\alpha$  effect (Rheinhardt & Brandenburg 2010). Finally, small-scale dynamo action is known to affect the negative effective magnetic pressure instability in hydromagnetic turbulence in the presence of strong density stratification; see Brandenburg et al. (2016) for a recent review of its theory and applications. Again, more systematic work in that direction is required and would benefit from the assurance that the dynamo effect is itself not being affected by the forcing details on the scale of the simulation domain. However, looking for secondary instabilities, such as the negative effective magnetic pressure instability or the large-scale dynamo instability, obviously requires continued care.

## ACKNOWLEDGEMENTS

We thank the referee for inspiring comments that have led to improvements in the paper. This work was supported through the FRINATEK grant 231444 under the Research Council of Norway, the Swedish e-Science Research Centre, the National Science Foundation, grant AAG-1615100, the University of Colorado through its support of the George Ellery Hale visiting faculty appointment, and the grant “Bottlenecks for particle growth in turbulent aerosols” from the Knut and Alice Wallenberg Foundation, Dnr. KAW 2014.0048. The simulations were performed using resources provided by the Swedish National Infrastructure for Computing (SNIC) at the Royal Institute of Technology in Stockholm and Chalmers Centre for Computational Science and Engineering (C3SE).

## REFERENCES

- Bhat, P., & Subramanian, K. 2013, MNRAS, 429, 2469  
 Bhat, P., Subramanian, K., & Brandenburg, A. 2016, MNRAS, 461, 240  
 Biskamp, D., & Müller, W.-C. 2000, Phys. Plasmas, 7, 4889  
 Boldyrev, S., & Cattaneo, F. 2004, Phys. Rev. Lett., 92, 144501  
 Boldyrev, S., Cattaneo, F., & Rosner, R. 2005, Phys. Rev. Lett., 95, 255001  
 Brandenburg, A. 2011, ApJ, 741, 92  
 Brandenburg, A., & Subramanian, K. 2005, Phys. Rep., 417, 1  
 Brandenburg, A., Rädler, K.-H., Rheinhardt, M., & Subramanian, K. 2008, ApJ, 687, L49  
 Brandenburg, A., Rogachevskii, I., & Kleorin, N. 2016, New J. Phys., 18, 125011  
 Brandenburg, A., Sokoloff, D., & Subramanian, K. 2012, Spa. Sci. Rev., 169, 123  
 Cattaneo, F. 1999, ApJ, 515, L39  
 Dobler, W., Haugen, N. E. L., Yousef, T. A., & Brandenburg, A. 2003, Phys. Rev. E, 68, 026304  
 Donzis, D. A., & Sreenivasan, K. R. 2010, J. Fluid Mech., 657, 171  
 Eyink, G. L. 2010, Phys. Rev. E, 82, 046314  
 Falkovich, G. 1994, Phys. Fluids, 6, 1411  
 Federrath, C., Chabrier, G., Schober, J., Banerjee, R., Klessen, R. S., & Schleicher, D. R. G. 2011, Phys. Rev. Lett., 107, 114504  
 Federrath, C., Schober, J., Bovino, S., & Schleicher, D. R. G. 2014, ApJ, 797, L19  
 Haugen, N. E. L., & Brandenburg, A. 2006, Phys. Fluids, 18, 075106  
 Haugen, N. E. L., Brandenburg, A., & Dobler, W. 2004, Phys. Rev. E, 70, 016308  
 Haugen, N. E. L., Brandenburg, A., & Mee, A. J. 2004, MNRAS, 353, 947  
 Isakov, A. B., Schekochihin, A. A., Cowley, S. C., McWilliams, J. C., Proctor, M. R. E. 2007, Phys. Rev. Lett., 98, 208501  
 Kaneda, Y., Ishihara, T., Yokokawa, M., Itakura, K., & Uno, A. 2003, Phys. Fluids, 15, L21  
 Käpylä, P. J., Käpylä, M. J., & Brandenburg, A. 2018, Astron. Nachr., 339, 127  
 Kazantsev, A. P. 1968, Sov. Phys. JETP, 26, 1031  
 Kleorin, N., & Rogachevskii, I. 2012, Phys. Scr., 86, 018404  
 Kulsrud, R. M., & Anderson, S. W. 1992, ApJ, 396, 606  
 Meneguzzi, M., Frisch, U., & Pouquet, A. 1981, Phys. Rev. Lett., 47, 1060  
 Moffatt, H. K. 1978, Magnetic Field Generation in Electrically Conducting Fluids (Cambridge: Cambridge Univ. Press)  
 Rheinhardt, M., & Brandenburg, A. 2010, A&A, 520, A28  
 Rogachevskii, I., & Kleorin, N. 1997, Phys. Rev. E, 56, 417  
 Schekochihin, A. A., Cowley, S. C., Hammett, G. W., Maron, J. L., & McWilliams, J. C. 2002, New J. Phys., 4, 84  
 Schekochihin, A. A., Cowley, S. C., Maron, J. L., McWilliams, J. C. 2004, Phys. Rev. Lett., 92, 054502  
 Schekochihin, A. A., Haugen, N. E. L., Brandenburg, A.,



- Cowley, S. C., Maron, J. L., & McWilliams, J. C. 2005, ApJ, 625, L115
- Schekochihin, A. A., Iskakov, A. B., Cowley, S. C., McWilliams, J. C., Proctor, M. R. E., & Yousef, T. A. 2007, New J. Phys., 9, 300
- Schober, J., Schleicher, D., Bovino, S., & Klessen, R. S. 2012, Phys. Rev. E, 86, 066412
- She, Z.-S., & Jackson, E. 1993, Phys. Fluids, A5, 1526
- She, Z.-S., Leveque, E. 1994, Phys. Rev. Lett., 72, 336
- Subramanian, K. 1999, Phys. Rev. Lett., 83, 2957
- Subramanian, K., & Brandenburg, A. 2014, MNRAS, 445, 2930 (SB14)
- Sur, S., Bhat, P., & Subramanian, K. 2018, MNRAS, 475, L72
- Thaler, I., & Spruit, H. C. 2015, A&A, 578, A54
- Tsuji, Y. 2004, Phys. Fluids, 16, L43